J Appl Electrochem (2010) 40:911–920
DOI 10.1007/s10800-009-9969-0

ORIGINAL PAPER

EIS measurements in the diagnosis of the environment within a PEMFC stack

S. Rodat · S. Sailler · F. Druart · P.-X. Thivel · Y. Bultel · P. Ozil

Received: 17 November 2008 / Accepted: 10 August 2009 / Published online: 25 August 2009

Abstract The diagnosis of flooding or drying is an important factor in improving the reliability and durability of PEMFCs. Indeed, flooding and drying lead to a reduction in the output voltage delivered by the fuel cell. Among the various diagnostic techniques, electrochemical impedance spectroscopy (EIS) is a powerful tool. In this study, EIS measurements were carried out on a 500 W stack comprised of 16 elementary cells. Electrochemical impedance spectra were recorded either on each cell or on the stack. Use of an electrical equivalent circuit model revealed that flooding mainly affects the transfer resistance and the cathodic Warburg impedance. A diagnostic tool based on these two components is proposed.

Keywords PEMFC · EIS · Water management · Diagnosis

1 Introduction

The Proton Exchange Membrane Fuel Cell (PEMFC) is one of the most attractive energy conversion devices, to be used in particular as a power source for stationary and mobile applications (stationary power generation, small portable applications, powering cars…). However, water management is a key issue in obtaining satisfactory and stable PEMFC performance [1, 2]. PEMFC durability and reliability are strongly dependent on water content. Suitable hydration of the membrane is therefore required to avoid both drying and flooding.

Water management of an MEA is quite complex. Water is produced within the cathode through the O_2 reduction reaction, while water transport takes place through the membrane. Water is transported from anode to cathode by electro-osmosis drag. Each proton crosses the membrane in a solvation shell. This phenomenon thus involves a water flow from the anode to the cathode. Water diffusion or back diffusion then occurs owing to the water concentration gradient on both sides of the membrane. In addition, water can be supplied to H_2 or O_2 flows by external humidifiers and removed as liquid or vapour by gas channels.

Among the various parameters, inlet gas flow rates can have a considerable influence on drying or flooding phenomena. Drying generally occurs when there are high water removal rates, generally obtained with a high overstoichiometric coefficient and a high temperature. The resulting decrease in membrane ionic conduction then results in significant ohmic loss. On the other hand, flooding occurs when the water production rate exceeds the water removal rate, resulting in water accumulation within the cell, particularly on the cathodic side. These conditions generally occur for low overstoichiometric coefficients. Water can accumulate in both the electrode and the gas channel. On the one hand, excess water in the electrode pores causes flooding that hinders oxygen diffusion in the porous volumes of both the gas diffusion layer and the active layer. Thus a reduction in the active area may be observed. On the other hand, water droplets can block the gas flow in the channels. The effect of either flooding or drying is reduced cell output voltage caused respectively by an increase in the cathodic overpotential or the ionic

S. Rodat · S. Sailler · F. Druart · P.-X. Thivel (✉) · Y. Bultel · P. Ozil
Laboratoire d'Electrochimie et de Physico-Chimie des Matériaux et des Interfaces (LEPMI), UMR 5631, CNRS-INPG, UJF, Domaine Universitaire, 1130, rue de la piscine, BP75, 38402 Saint-Martin d'Héres Cedex, France
e-mail: pierre-xavier.thivel@ujf-grenoble.fr

ohmic drop losses. Therefore an accurate diagnosis of fuel cell stack water management is important for the development of industrial applications for PEMFC technology.

The aim of this study is to characterise PEMFC flooding or drying using electrochemical impedance spectroscopy (EIS). Electrochemical Impedance Spectroscopy has been demonstrated to be a powerful non-invasive in situ experimental technique for investigating the complex processes occurring within a PEMFC [3]. EIS has been used to study intraelectrode processes within thin porous coating electrodes and gas diffusion electrodes in a half cell [4–8] and suitable models were developed to interpret the experimental results. More recently, impedance techniques have been used to study the response of a complete single cell [9–13]. Based on a detailed description of transport phenomena in a Gas Diffusion Electrode, a pertinent explanation was proposed by Paganin et al. [9] for the impedance diagrams of a PEMFC. Their main conclusions concern the important roles of water transport within the membrane and oxygen diffusion within the gas diffusion layer of the electrode, particularly when using air rather than pure oxygen. Freire and Gonzalez [10] studied the impedance response of a H_2/O_2 PEMFC under different working conditions and with several Nafion membrane thicknesses. Their results clearly highlighted that thinner membranes (<100 μm) offer better characteristics for water management, because of a much lower sensitivity to temperature and current density changes. Song et al. [11] optimized the electrode structure and composition, using information from the cell current-potential and AC impedance measurements. Wagner [12] simulated experimental impedance diagrams by using an equivalent circuit and taking into account electrode impedances and electrolyte resistance. Andreaus et al. [13] investigated performance loss in a PEMFC operating at high current densities. These authors explain their experimental results on the basis of a shortage of water within the membrane, which leads to decreased membrane conductivity and increased activation potential for the hydrogen oxidation reaction. These effects are due to a decrease in the number of active sites on the anodic side.

AC impedance measurements have mainly been used to determine the internal resistance of such systems, which is partly related to membrane resistance. This resistance depends on water content and fuel cell temperature. Merida et al. [14] and Le Canut et al. [15] used EIS to detect membrane drying or flooding respectively for a four-cell stack and for a 4-22 cells stack. An increase in the impedance value was observed under flooding conditions compared to optimal conditions. More recently Roy and Orazem [16] coupled impedance spectroscopy with a measurement-model-based error analysis to detect the onset of flooding in a single PEM fuel cell. Moreover, Fouquet et al. [17] proposed a model of AC impedance measurements for monitoring the state-of-health of a 150 cm^2 six-cells PEMFC, by studying variations in the parameters of a Randles-like equivalent circuit as a function of flooding or drying conditions.

Thus, EIS is a powerful tool used to characterise and to perform the state of health of a PEMFC stack as in few studies [14, 15, 17–19]. The aim of the present study is to identify and characterise a 100 cm^2 16-cells PEMFC stack flooding or drying by using EIS and to diagnose the flooding or drying mechanisms for a stack through a suitable model. Moreover, in this study EIS measurement of each cell of the stack and EIS of the overall stack is compared in order to find a tool for rapid non-intrusive diagnostic. Thanks to EIS method and model, it is then possible to detect a defect or failure in the stack due to one cell, while the other cells work correctly.

2 Experimental set-up and modelling

The experimental data of this study were obtained on a 500 W PEMFC stack. This stack comprised 16 cells composed of 100 cm^2 membrane electrode assemblies (MEA) supplied by Paxitech®. The MEAs were made of Nafion® membrane (thickness 50 μm) and a gas diffusion electrode. The platinum loads of the Paxitech® electrodes were 0.6 mg/cm^2 for both anode and cathode. The cells were fed with pure hydrogen and oxygen. The stack temperature was controlled by means of a thermostatic bath. The inlet and outlet cell temperatures were measured by thermocouples during the whole experiment and their variations did not exceed 2 K around the set point. The cells were purged between two runs or after flooding on both cathode and anode sides by using pure nitrogen. The fuel cell test bench (Fig. 1) was operated by a Schneider Electric Premium system that independently controlled fluid and electrical circuits and guaranteed the safety of the experiment. The pressure in each compartment was automatically controlled at 2 bars. The trials were performed in galvanostatic mode using an Agilent N3300A electronic load with two N3306A modules (0–120 A, 0–60 V, 600 W).

Impedance measurements were carried out using an Autolab PGSTAT302 potentiostat with an Autolab FRA2 module (frequency response analyser) combined with the Agilent electronic loads. The loads 1 and 2 are connecting in parallel on the stack. The AC signal amplitude was about 10% of operating current (for 50 A, a signal about ±2.5 A around 50 A) and the frequency range from 5 kHz to 0.5 Hz was covered by 50 points. The current is modulated through the stack and the voltage is measured either across a single cell (EIS of cell) either across the stack (EIS of the stack). The AC signal amplitude was optimized for this

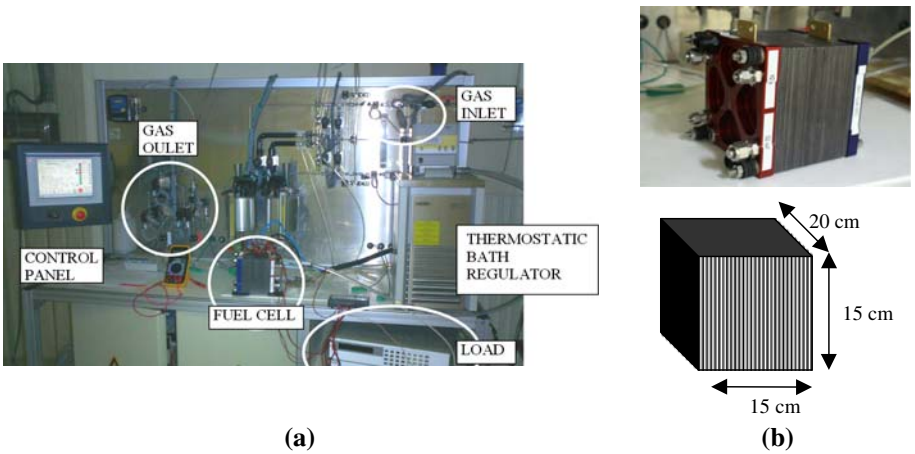

Fig. 1 Test bench (**a**) and PEMFC stack (**b**)

study at high current. Figure 2 presents the corresponding device scheme. The time between each EIS measurement was about 2 min and each cell EIS measurement was recorded successively.

EIS spectra were determined for both the entire stack and each cell at several temperatures and overstoichiometries. Different behaviours of the stack were thus analyzed for standard, drying and flooding conditions. The hydrogen compartment was in dead-end mode for each run.

The PEMFC stack was operated in running conditions for half an hour to achieve steady state conditions before starting each EIS measurement.

The electrochemical behaviour of the MEA was simulated by describing it as a suitable equivalent circuit that involves various impedance components representing the various electrochemical steps (Fig. 3).

The physical model used to obtain the following governing equation for PEMFC responses is based on a previous d.c. and a.c. model [20]. In the absence of mass transport limitation, the electrochemical reaction is simply represented by an equivalent electrical circuit of parallel RC cells. However when significant variations in the interfacial concentrations on the electrodes occur, the electrochemical reaction is represented by an equivalent circuit with parallel Z_f, C [15]. The faradaic impedance Z_f is composed of two impedances in series: a charge transfer resistance R_t and an impedance related to the diffusion of reduced species on the cathode side or oxidized species on the anode side. This diffusion impedance is called the Warburg impedance and is represented by Z_W. But the complete description of the electrode impedance must account for the double layer capacitance (C_{dl}). The

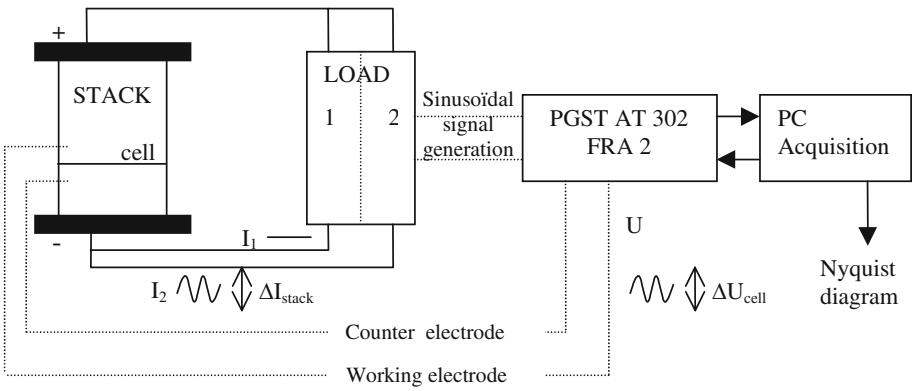

Fig. 2 Device scheme of the EIS measurement

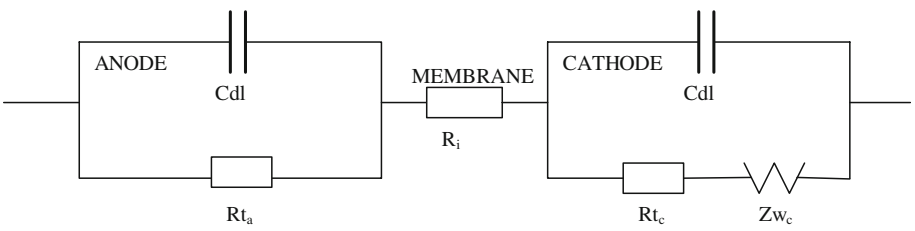

Fig. 3 Equivalent electrical model of the PEMFC

impedance of an electrode then corresponds to the parallel combination of the faradic impedance Z_f and the double layer capacitance to describe the dynamics of the changing concentration in the gas backing layer and the charge stored in the interfacial capacitance. On the cathode side, oxygen gas transport limitation can occur due to water flooding, while hydrogen gas diffusion is generally assumed negligible with regard to the other phenomena. The anode equivalent circuit thus involves the double layer capacitance (C_{dl}) and the transfer resistance related to electron transfer (R_{ta}). The corresponding impedances are then expressed as:

$$Z_{\text{cathode}}(\omega) = \frac{1}{1/(R_{tc} + Z_{Wc}(\omega)) + j\omega C_{dl}} \quad (1)$$

and

$$Z_{\text{anode}}(\omega) = \frac{1}{1/(R_{ta}) + j\omega C_{dl}} \quad (2)$$

Note that the Membrane Electrode Assembly design is symmetric. The same type of electrode and Pt/C catalyst loading are considered for both anode and cathode. The double layer capacitance (C_{dl}) is quite similar and thus assumed equal for both electrodes.

In the frequency domain, a restricted diffusion impedance, assuming a Fick's law, thus allows approximation of the contribution of oxygen mass transport within the gas diffusion layer on the cathode side. An approximation of the Warburg impedance [20] is given by:

$$Z_{Wc}(\omega) = \frac{A_c}{\sqrt{1 + j\omega t_c}} \quad (3)$$

where t_c is the diffusion time constant (s) and A_c the Warburg constant (Ohm).

The total impedance of the fuel cell is composed of two impedances (one per electrode), in series with the internal resistance R_i linked to the membrane (Fig. 3). Finally, the MEA equivalent circuit includes the two models of electrodes in series with the internal resistance:

$$Z_{\text{MEA}}(\omega) = Z_{\text{anode}}(\omega) + R_i + Z_{\text{cathode}}(\omega) \quad (4)$$

It is worth mentioning that the internal resistance (R_i) is related to the membrane resistance (R_m) and also contact resistances.

This classical model was selected in order to describe the cells within the stack. It offers a suitable approach in order to identify the real phenomena and allow a fast diagnosis of the stack. In the present case, the stack involves 16 elementary cells assumed to be equivalent and consequently its impedance is:

$$Z_{\text{Stack}}(\omega) = 16 \cdot Z_{\text{MEA}}(\omega) \quad (5)$$

Based on these EIS models of the MEA and stack, a procedure was performed to fit the real and imaginary parts of the experimental impedances obtained for the cell and the stack. Five parameters were thus used to fit the simulated and experimental impedances: R_{ta}, R_{tc}, C_{dl}, t_c, A_c. For consistency, the internal resistance R_i value used in the model is the experimental resistance value measured at high frequency.

Impedance data were fitted using the Matlab optimization toolbox (LSQCURVEFIT function) using Gauss-Newton line-search method algorithm for non-linear least-square problem solving. The experimental data obtained at low frequency were not used for curve fitting because measurement uncertainty was too great. The EIS diagrams were fitted in a frequency range from 5 kHz to 3 Hz.

3 Results and discussion

The experimental study is divided into two parts. The first part presents the experimental EIS diagrams for each cell and their fitting by the model previously described. The goal here is to detect the operating conditions leading to flooding either in a single cell or in several cells and to determine which parameter is significantly influenced by water accumulation.

The second part is devoted to the study of measured and fitted overall EIS diagrams for the stack for different operating conditions (standard, flooding or drying) and to the final diagnosis of the stack by measuring only one impedance spectrum.

3.1 Study of the flooding of a cell

In this first part, the behaviour of the stack was investigated at 50 °C for a 50 A fixed current with a feed of pure hydrogen at the anode and pure oxygen with 3 different overstoichiometric coefficients at the cathode. Experimental impedance spectra highlighted a heterogeneous behaviour of the cells. Two cells (number 7 and 13) were selected for their specific electrochemical behaviours. Note that the EIS measurements were performed before purging the fuel cell stack with pure nitrogen (runs 1 and 2) and afterwards (runs 3 and 4) as shown in Fig. 4. Figure 5

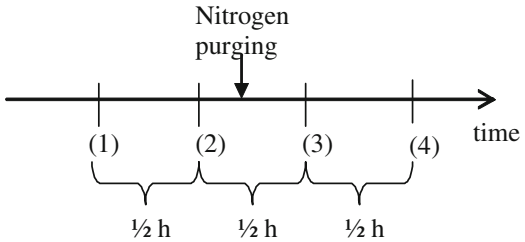

Fig. 4 Experimental running

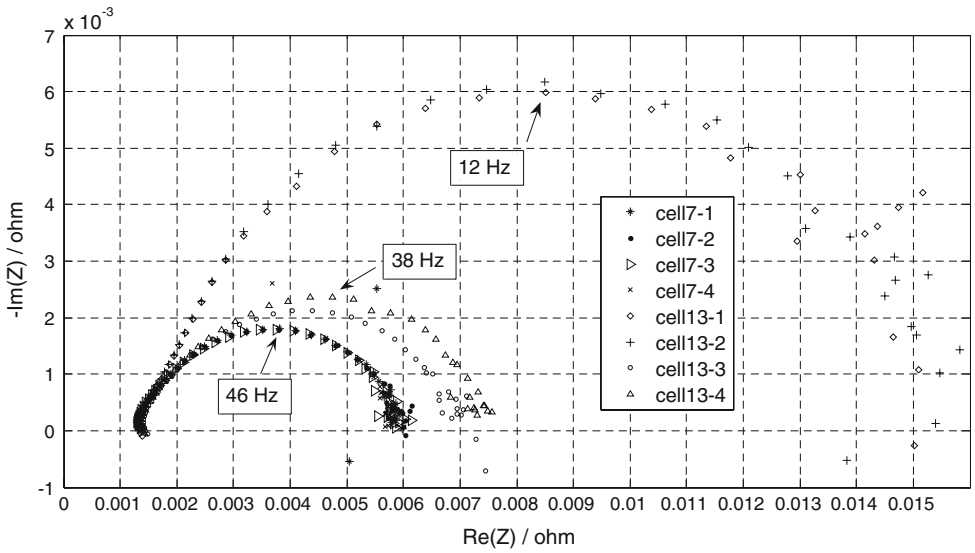

Fig. 5 Experimental impedance diagrams

presents typical experimental impedance spectra in the Nyquist plot on both cells for runs (1) to (4). The capacitive loop recorded between 1000 and 0.1 Hz is characteristic of the contribution of fuel cell interfaces to impedance. The separation between the charge transfer resistance and diffusion arcs does not appear due to the very large value of the double layer capacitance.

An analysis of these experimental impedance diagrams for the H_2/O_2 PEMFC can be performed based on the model presented in Sect. 2 of this study. Even though the effects of kinetics and mass transport in the GDL are partly superimposed in the impedance spectra, the experimental results were analysed for the purpose of elucidating the mass-transport phenomena within the gas diffusion electrode, which give rise to low-frequency features in the impedance spectra.

Impedance spectra (7-1, 7-2, 13-1, 13-2) and (7-3, 7-4, 13-3, 13-4) were respectively recorded before and after purging. In our operating conditions, diagrams for cell 13 appear significantly larger than those for cell 7 before purging. After nitrogen purging, the spectrum amplitude clearly decreases for cell 13 whereas it remains relatively unchanged for cell 7. Replications were then performed leading to spectra 7-4 and 13-4.

This behaviour could be related to electrode flooding. The water produced by the electrochemical reaction was assumed to be liquid and its effect was taken into account through a homogeneous decrease in the gas diffusion electrode porosity. In addition, we also assumed that this liquid water partly blocked the electrode geometrical surface area, reducing the reactive area. Between the trials before and after purging, cell flooding is confirmed: the spectrum amplitude is increased in flooding conditions as previously reported in the literature [15] and the spectrum modification seems reversible (Fig. 5).

On the basis of this experimental investigation, it can be stated that both polarisation resistance (i.e. the charge transfer resistance and the Warburg impedance) and apex frequency should be criteria for diagnosing the flooding state of a cell, but it is necessary to scan the entire spectrum range.

The impedance spectra obtained by EIS provided a set of model parameters. Figure 6 shows the good agreement between experimental and fitted impedance diagrams, using the model parameter values shown in Table 1. The variations in the fitted parameters are presented in Fig. 7a and b respectively for cell 7 and cell 13. As expected, the three parameters, R_{tc}, A_c and t_c turn out to be more sensitive to the flooding effect than the others (R_{ta}, R_i and C_{dl}). The same behavior is observed in [17] where two parameters are particular affected by the flooding: the polarization and the diffusion related resistances. In the case of a optimal cell (cell 7) the apex frequence still remain around 46 Hz with time whereas in case of the flooding cell (cell 13) the apex frequence increased from 12 to 38 Hz after the nitrogen purging. A low frequency could thus possibly indicate flooding. On the other hand, the internal resistance was only slightly modified by flooding and a mean value about 0.0013 Ω was measured. The membrane can thus be considered to have similar humidification conditions. No significant variation was observed for cell 7 which operated under standard conditions, except for parameter t_c in the Warburg impedance. In the case of cell 13, initially under flooding condition (13-1, 13-2) then purged with nitrogen (13-3, 13-4), all the parameters were affected by the flooding.

It appears that the charge transfer resistance and the Warburg impedance on the cathodic side were the parameters most affected. Accordingly, for cell 13, parameters R_{tc}, and A_c are three times lower after purging. In fact the

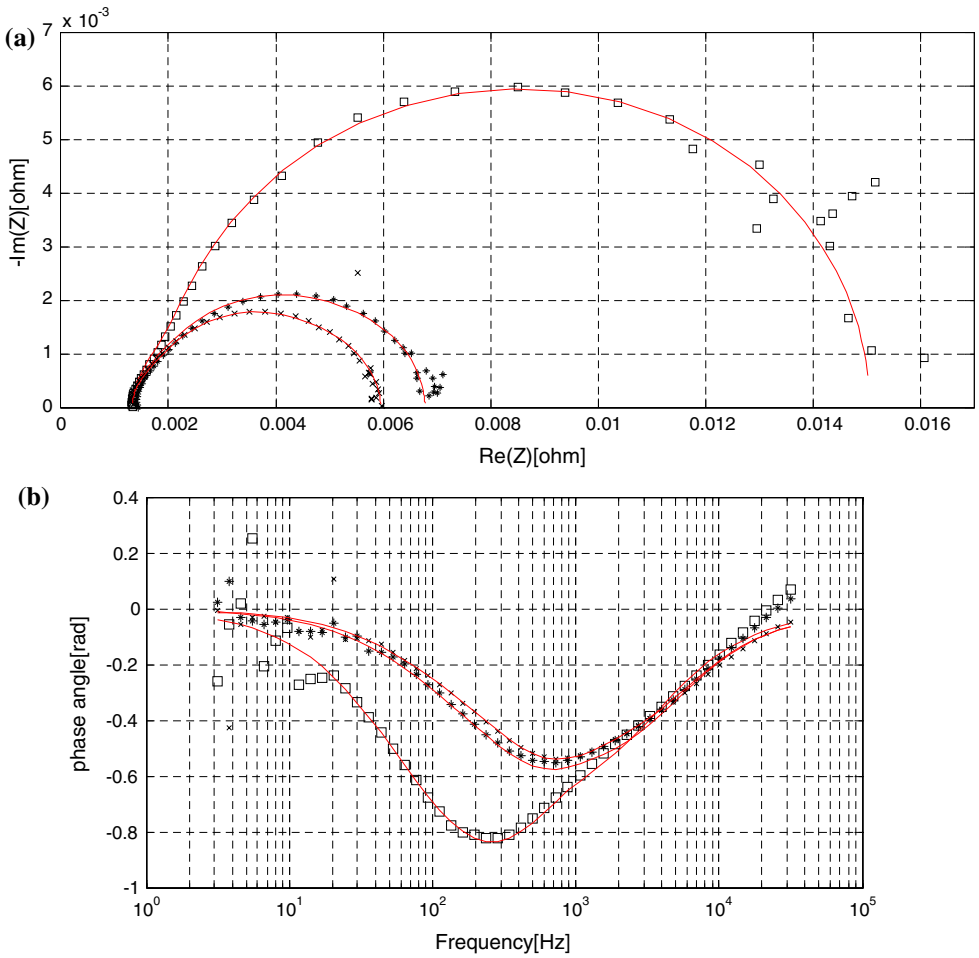

Fig. 6 Impedance spectra fitting in Nyquist plot (**a**) and phase angle in Bode plot (**b**): trial 1 with a flooded cell (*open square* cell 13-1) and a standard cell (*multi symbol* cell 7-1) and trial 3 after nitrogen purge (*asterisk* cell 13-3) *line* simulated diagrams

Table 1 Fitting parameters used for the model

	Cell 7-1	Cell 7-2	Cell 7-3	Cell 7-4	Cell 13-1	Cell 13-2	Cell 13-3	Cell 13-4
R_i (10^{-3} ohm)	1.30	1.30	1.31	1.31	1.33	1.31	1.41	1.37
R_{ta} (10^{-4} ohm)	5.02	5.18	4.92	5.23	6.93	6.14	6.02	5.92
R_{tc} (10^{-3} ohm)	3.01	3.02	2.94	2.93	9.69	8.90	3.47	3.43
C_{dl} (10^{-3} Farad)	7.57	7.71	7.74	7.78	9.06	8.69	7.52	7.39
t_c (10^{-2} s)	1.32	1.31	1.01	0.81	2.24	1.46	1.33	0.99
A_c (10^{-3} ohm)	1.11	1.05	1.07	1.02	3.35	4.02	1.38	1.93

cathodic Warburg impedance describes the interaction between flooding and oxygen transport limitation. Both R_{tc} and A_c thus increased when the water content was increased. It is worth mentioning that t_c was also affected by flooding.

The double layer capacitance mainly depends on the physical design of the MEA and therefore is not really affected by the water amount.

Water seems to have a more important effect on the cathodic parameters. The cathodic production of water leads to water accumulation that prevents the gas from reaching the electrode. It can be related to the decrease in porosity of the gas diffusion electrode. When nitrogen purging was carried out, the cathode charge transfer resistance decreased to a value close to that of cell 7, indicating a clear relation between the cathode charge transfer resistance and flooding. In the case of cell 7, no effect of nitrogen purging was observed showing that this cell was not able to accumulate water. These results are in agreement with those of Fouquet et al. [17] for a 150 cm^2 six-cell air/H_2 PEM where a set of three parameters of their Randles model with CPE exhibiting a high sensitivity to flooding or drying: the membrane resistance, the polarisation resistance and the diffusion resistance.

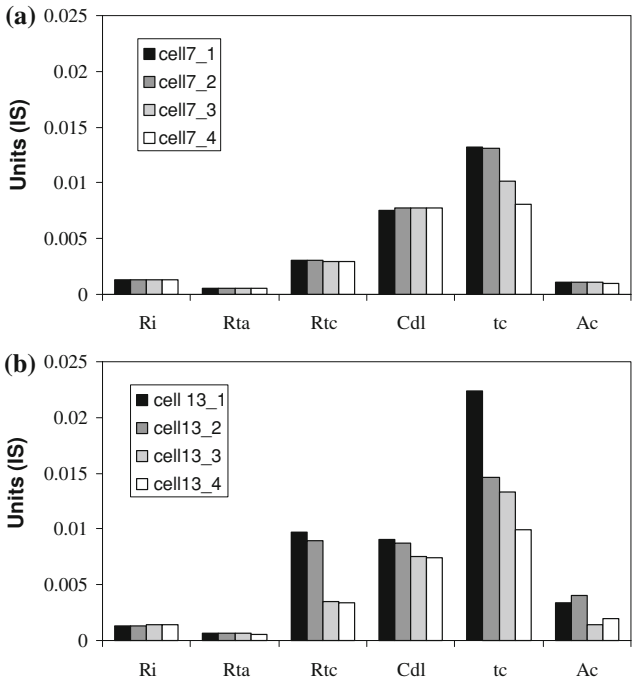

Fig. 7 Fitting parameters for a standard cell (**a**) and a flooded cell (**b**)

3.2 Study of the flooding of a stack

The study on the stack was designed to obtain a diagnosis without measuring each cell spectrum but from an overall measurement on the 16-cell stack. As underlight in [14] the overall stack impedance seem to be more interesting for the implementation of a diagnostic device. Different operating conditions were tested with varying voltage set-points, as shown in Fig. 8.

Twelve experiments were carried out:

- Trials (1–5) under standard conditions: 50 A, 50 °C, O_2 feed with an overstoichiometric coefficient equal to 1.5
- Trials (6–7) under flooding conditions: 50 A, 40 °C (low temperature) in order to decrease water removal.
- Trials (8–12) under drying conditions: 50 A, higher temperature (50 °C and 60 °C) and high oxygen feed (O_2 overstoichiometry 6) in order to increase water removal.

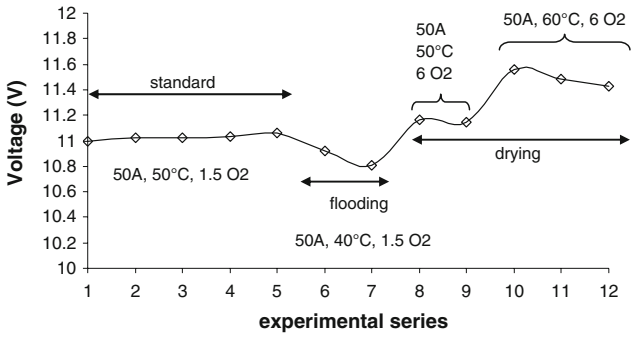

Fig. 8 Working conditions on the 500 W stack and set-point variation

The time between each trial was about 15 min.

Figure 9 presents the experimental and simulated impedance spectra of the whole stack corresponding to the second trails of each series ((2) (7) (9) and (11)).

Table 2 presents the parameters deduced from fitting and the internal resistance determined at the intersection of the high frequency limit with the real axis.

Figure 10 shows the evolution of these parameters. The internal resistance remains low. Its average value close to 0.0015 Ω is slightly modified by humidification conditions and quite similar to that measured on a single cell during the previous trials. Hence increasing water removal did not enable drying conditions to be reached for trials 8–12. A comparison between trials (2) and (9) reveals similar behaviour. Water accumulated during experiments (6) and (7) is removed by increasing both oxygen feed flow and stack temperature.

For experiment 7 in flooding conditions, higher values of R_{tc} and A_c bear out the previous conclusion for the cell impedance analysis. The resistance R_{tc} and the Warburg parameter A_c appear to be the more relevant parameters for detecting flooding for a cell as well as for a stack.

The stack temperature influences R_{tc}, which decreases when temperature increases. The results show that the evolution of R_{tc} is more significant when the temperature is decreased to 40 °C than when it is increased up to 60 °C. This observation confirms that R_{tc} evolution can be attributed to cell flooding for trials 6 and 7 at 40 °C.

The variations in R_{tc} and A_c are smaller for the stack than between the cells. In fact, parameter values here are the average for 16 cells because of the equivalent model chosen. Heterogeneous behaviour of each cell contributes to the attenuation of the evolution of the parameters. Nevertheless, for experiment 7, the average value of R_{tc} is higher than the previous value for a standard cell (cell 7): 4.15×10^{-3} Ω for the stack in experiment 7 compared with 2.98×10^{-3} Ω for cell 7.

3.3 Diagnostic tool

Table 3 summarizes the values of the parameters of the model obtain respectively in the case of a standard cell, a flooded cell and the a flooded stack.

Increases in parameters t_c, R_{tc} and A_c are observed for both cell and stack flooded. Nevertheless, the increases for the stack are smaller due to the assumed uniform distribution of the flooding in the 16 cells. Finally, relative deviations between flooded cell or flooded stack

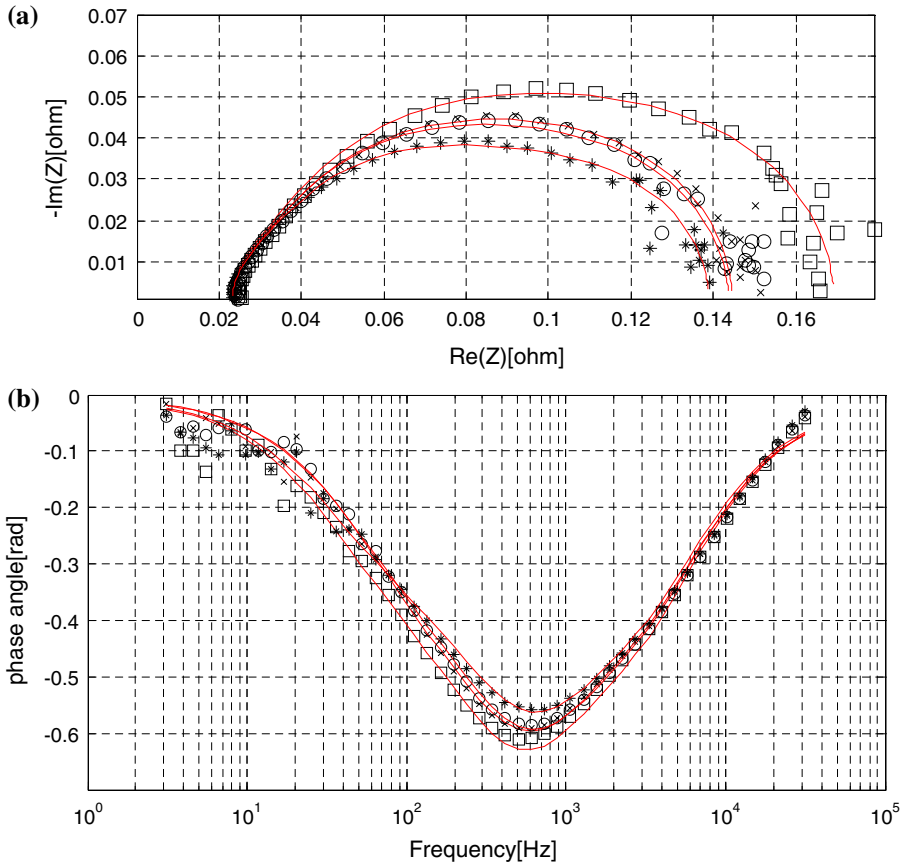

Fig. 9 Experimental and simulated impedance diagrams for the stack in Nyquist plot (**a**) and phase angle in Bode plot (**b**) (*multi symbol* trial 2, *open square* trial 7, *open circle* trial 9, *asterisk* trial 11, *line* fitted stack model)

Table 2 Stack model parameters for each trial

	1	2	3	4	5	6	7	8	9	10	11	12
R_i (10^{-3} ohm)	1.52	1.49	1.49	1.48	1.48	1.52	1.54	1.49	1.49	1.49	1.45	1.44
R_{ta} (10^{-4} ohm)	5.92	5.90	6.25	6.49	5.89	6.61	6.65	6.50	6.12	6.20	5.80	5.95
R_{tc} (10^{-3} ohm)	3.97	3.98	4.32	4.46	4.02	4.53	4.66	4.32	4.01	3.60	3.55	3.62
C_{dl} (10^{-3} Farad)	6.18	6.14	6.33	6.47	6.01	6.06	5.99	6.41	6.12	7.05	6.41	6.50
t_c (10^{-2} s)	1.62	1.53	2.19	2.37	1.66	2.07	2.30	2.62	1.72	2.60	2.39	2.19
A_c (10^{-3} ohm)	2.90	3.02	3.02	2.82	3.30	3.54	3.81	2.82	2.91	2.78	3.10	2.89

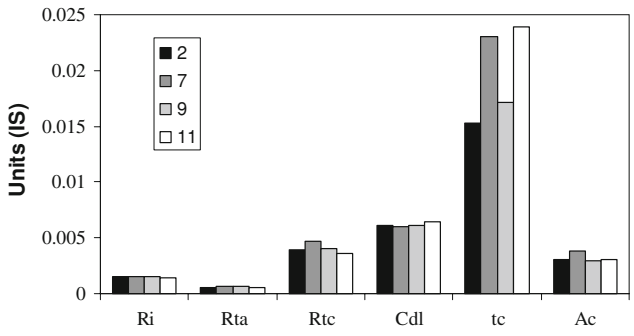

Fig. 10 Model parameters

and standard cell are represented in Fig. 11. A deviation up to 50% is obtain respectively on t_c, R_{tc} and A_c parameters.

Table 3 Comparison of the fitting parameters for a flooded cell, a flooded stack and standard cell

	Standard cell	Flooded cell	Flooded stack
R_i (10^{-3} ohm)	1.31	1.32	1.53
R_{ta} (10^{-4} ohm)	5.09	6.53	6.63
R_{tc} (10^{-3} ohm)	2.98	9.30	4.60
C_{dl} (10^{-3} Farad)	7.70	8.88	6.02
t_c (10^{-2} s)	1.11	1.85	2.19
A_c (10^{-3} ohm)	1.06	3.68	3.68

The large increase in parameters t_c, R_{tc} and A_c that is observed in all the cases can be explained by flooding. Flooding implies an increase in the charge transfer resistance at the cathode and in the Warburg impedance due to

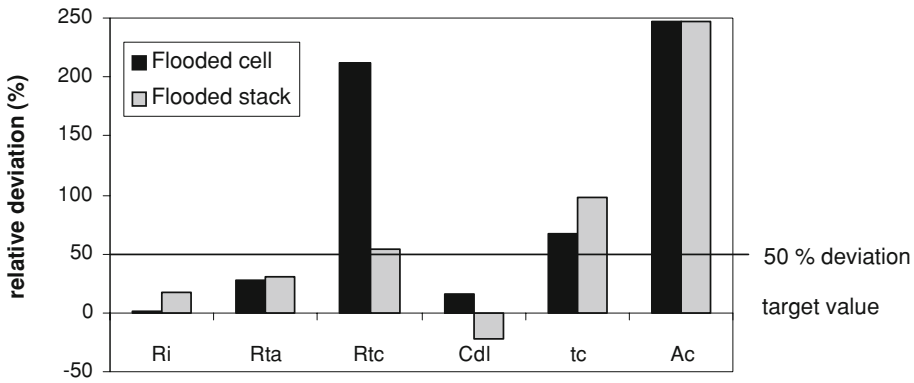

Fig. 11 Relative deviation to standard values

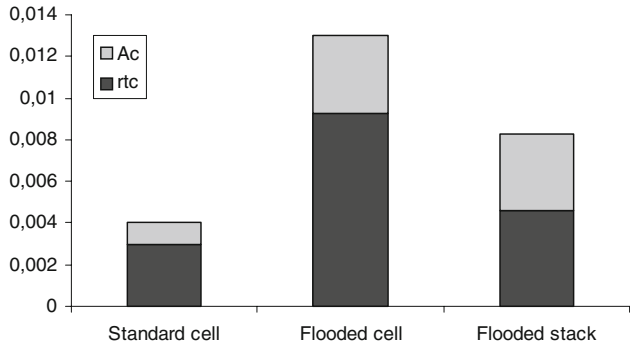

Fig. 12 Diagnostic tool

the appearance of water that reduces the surface available for the reaction and limits oxygen diffusion.

Flooding is characterised by an increase in the diameter of the impedance arc. This diameter is equal to the sum of the charge transfer resistance and the real part of the Warburg impedance. For a frequency close to zero, this real part is equal to A_c (according to the simplified expression of the Warburg impedance adopted in our study). The increase in the arc diameter is thus due to the increase in R_{tc} and A_c. The disadvantage of the overall EIS measurement of a stack is the resulting smoothing of the characteristic values, as underlined by Table 3. The impact of flooding on the charge transfer resistance and on the real part of the Warburg impedance is thus under-estimated. In order to overcome this problem, it is possible to add these two parameters in order to improve the detection of flooding as shown in Fig. 12.

Nevertheless, using a simple model enables identification of a flooding phenomenon by measuring impedance at low frequency and comparing it with that of a reference cell operating under standard conditions.

4 Conclusions

This article discusses the diagnosis of a PEMFC by means of EIS measurements. It focuses particularly on the problem of water management in the fuel cell. EIS measurements were successfully performed for a 500 W stack and for each of its 16 cells. Various operating conditions (different temperatures and overstoichiometric coefficients) were tested in order to include either flooding or drying. The effect of a nitrogen purge was also observed.

EIS applied to all the cells made it possible to clearly identify flooded cells. In such a situation, a cell-equivalent circuit allowed the effect of humidity to be highlighted, especially on the cathodic charge transfer resistance and the Warburg impedance. Moreover EIS measurements showed that a flooded cell could, after nitrogen purging, return to optimal operating conditions.

Furthermore, recording the overall impedance spectra of a stack and fitting them through an equivalent circuit allowed a diagnosis of the stack showing the same effect of humidity as for the cells.

EIS remains a relevant tool for rapid non-invasive diagnosis. It clearly appeared that measuring only two impedances respectively at low and high frequency makes possible a diagnosis of the stack behaviour in a short time.

References

1. Yousfi-Steiner N, Moçotéguy P, Candusso D et al (2008) J Power Sources 183:260
2. Li H, Tang Y, Wang Z et al (2008) J Power Sources 178:103
3. Selman JR, Lin YP (1993) Electrochim Acta 38:2063
4. Springer TE, Raistrick ID (1989) J Electrochem Soc 136:1594
5. Springer TE, Zawodzinski TA, Wilson MS et al (1996) J Electrochem Soc 143:587
6. Raistrick ID (1990) Electrochim Acta 35:1579
7. Eikerling M, Kornyshev AA (1999) J Electroanal Chem 475:107
8. Antoine O, Bultel Y, Durand R (2001) J Electroanal Chem 499:85
9. Paganin VA, Oliveira CLF, Ticianelli EA et al (1998) Electrochim Acta 43:3761
10. Freire TJP, Gonzalez ER (2001) J Electroanal Chem 503:57
11. Song JM, Cha SY, Lee WM (2001) J Power Sources 94:78
12. Wagner NJ (2002) J Appl Electrochem 32:859
13. Andreaus B, McEvoy AJ, Scherer GG (2002) Electrochim Acta 47:2223

14. Mérida W, Harrington DA, Le Canut JM et al (2006) J Power Sources 161:264
15. Le Canut JM, Abouatallah RM, Harrington DA (2006) J Electrochem Soc 153:A857
16. Roy SK, Orazem ME (2007) ECS Transactions 11:485
17. Fouquet N, Doulet C, Nouillant C et al (2006) J Power sources 159:905
18. Yuan X, Sun JC, Blanco M et al (2006) J Power Sources 161:920
19. Yan X, Hou M, Sun L, Liang D et al (2007) Int J Hydrog Energy 32:4358
20. Iftikhar U, Riu D, Druart F et al (2006) J Power Sources 160:1170